Joint Defragmentation of Optical Spectrum and IT Resources in Elastic Optical Datacenter Interconnections

Wenjian Fang, Minhua Lu, Xiahe Liu, Long Gong, and Zuqing Zhu

***Abstract*—With its agile spectrum management in the optical layer, the flexible-grid elastic optical network can become a promising physical infrastructure to efficiently support the highly dynamic traffic in future datacenter interconnections (DCIs). While the resulting elastic optical DCIs (EO-DCIs) need to serve requests that not only require bandwidth resources on fiber links but also require multidimensional IT resources in the DCs, multidimensional resource fragmentation can occur during dynamic network operations and deteriorate the network performance. To address this issue, this paper investigates the problem of joint defragmentation (DF) for the spectrum and IT resources in EO-DCIs. Specifically, we reoptimize the allocations of multidimensional resources jointly with complexity-controlled network reconfigurations. For the DF operation, we first study the request selection process and propose a joint selection strategy that can perform the spectrum- and IT-oriented selections adaptively according to the network status. Then, we formulate a mixed integer linear programming model and design several heuristics to tackle the problem of network reconfiguration in the joint DF. The proposed algorithms are evaluated with extensive simulations. Simulation results demonstrate that the proposed joint DF algorithms can significantly reduce the blocking probability in EO-DCIs by consolidating the spectrum and IT resource usages effectively.**

***Index Terms*—Elastic optical datacenter interconnections (EO-DCIs); Multi-dimensional resource defragmentation.**

I. Introduction

With the fast development of cloud computing, datacenter interconnections (DCIs) that connect geographically distributed datacenters (DCs) together across a wide-area network (WAN) have been deployed rapidly on large scales. It is known that the traffic demands in DCIs usually have various bandwidth requirements and their load can change significantly over time [1]. Hence, the network may exhibit the coexistence of huge peak throughput and high burstiness, which brings new challenges to the physical layer.

With the tremendous bandwidth in optical fibers, optical networking provides DCIs a viable infrastructure for carrying traffic cost-effectively [2]. Previously, researchers have studied the optical DCIs that are based on fixed-grid wavelength division multiplexing (WDM) networks [3–5]. However, it is known that with the fixed wavelength grids, these WDM networks may only provide limited flexibility on bandwidth provisioning in the optical layer [6–8]. Recently, elastic optical networks (EONs) that are enabled by new optical transmission and switching technologies have attracted significant attention, as they can provide super-channel capacity over Tb/s as well as spectrum allocation granularity at 12.5 GHz or less [6,7]. Different from the fixed-grid WDM networks, EONs operate on flexible wavelength grids, and hence can achieve agile spectrum management and provision requests with various bandwidth requirements more efficiently. Therefore, EON has been considered as a promising physical infrastructure for supporting future DCIs [9,10]. In [11], Klinkowski and Walkowiak compared the performance of DCIs that are based on WDM networks and EONs, and showed the advantages of elastic optical DCIs (EO-DCIs) in terms of spectrum utilization, network scalability, etc.

Note that agile spectrum management with fine spectrum granularity also makes the network control and management (NC&M) in EONs more complex. For instance, as an EON uses several spectrally contiguous frequency slots (FSs) to provision the bandwidth requirement of a lightpath request, setting up and tearing down lightpaths frequently can result in spectrum fragmentation [12,13]. Specifically, spectrum fragmentation induces nonaligned, isolated, and small-sized FS blocks in the optical spectra. As these FS blocks can hardly be used by future lightpaths, spectrum fragmentation limits the resource utilization in EONs and can degrade network performance significantly [13]. Considering the fact that DCIs have highly dynamic traffic demands and network operators need to provide bandwidth on demand, spectrum fragmentation will be

Manuscript received November 11, 2014; revised January 30, 2015; accepted February 16, 2015; published March 26, 2015 (Doc. ID 226521).

W. Fang, X. Liu, L. Gong, and Z. Zhu (e-mail: zqzhu@ieee.org) are with the School of Information Science and Technology, University of Science and Technology of China, Hefei, Anhui 230027, China.

M. Lu is with the National-Regional Key Technology Engineering Laboratory for Medical Ultrasound, Guangdong Key Laboratory for Biomedical Measurements and Ultrasound Imaging, Department of Biomedical Engineering, Shenzhen University, Shenzhen, Guangdong 518060, China.

http://dx.doi.org/10.1364/JOCN.7.000314

inevitable in EO-DCIs. In order to tackle the problem of spectrum fragmentation, previous studies have proposed a few defragmentation (DF) schemes that leveraged lightpath reconfiguration to consolidate spectrum usage [12–16].

On the other hand, the requests in EO-DCIs may not only need bandwidth resources on fiber links but also require multidimensional IT resources (e.g., CPU cycles, memory, and disk storage) in destination DCs [2]. If the IT resources are not properly allocated among the DCs, their usages can be unbalanced. Since the IT resources in each DC are multidimensional, unbalanced usage can lead to a situation in which the insufficiency of one type of IT resource makes the whole DC unusable, even though other types of IT resources are still plentiful. Since this mimics the issue of spectrum fragmentation, i.e., low utilization due to the fact that the available resources are not properly aligned in multiple dimensions, we refer to it as IT resource fragmentation [17]. Apparently, IT resource fragmentation can also degrade the performance of EO-DCIs significantly, especially for those whose DCs are relatively small with limited IT resources [18]. Note that applications such as cloud computing bear an attractive attribute of anycast [19]; i.e., the destination DC of a request is flexible. Also, the services in one DC can be migrated to another with virtual machine (VM) migrations. Inspired by the joint spectrum and IT resource allocation approaches developed for virtual optical network provisioning [10,20,21], we expect that by leveraging the joint DF that reoptimizes the spectrum usage on fibers and the IT resource allocations in DCs, one can operate EO-DCIs in a wiser way [22].

In this work, we investigate the problem of joint DF for the spectrum and IT resources in EO-DCIs. Specifically, in order to reduce the blocking probability in an EO-DCI, we reoptimize the allocations of the multidimensional resources jointly with complexity-controlled network reconfigurations. The network reconfiguration changes not only the routing and spectrum assignment (RSA) of lightpaths (as in DF for EONs [16]) but also the IT resource allocations in the DCs.

The rest of the paper is organized as follows. We describe the problem of joint DF for multidimensional resources in EO-DCIs in Section II. Section III presents the overall procedure of the joint DF, and discusses the request selection strategy for network reconfiguration. The network reconfiguration is studied in Section IV, in which we formulate a mixed integer linear programming (MILP) model and propose several heuristic algorithms. We present the performance evaluation in Section V. Finally, Section VI summarizes the paper.

II. Problem Formulation

In this section, we first describe the network model that is used to investigate the joint DF, and then discuss the problem of multidimensional resource fragmentation in EO-DCIs.

A. Network Model

We consider the physical topology of the EO-DCI as a directed graph $G(V,E)$, where V and E represent the sets of nodes and fiber links in the network, respectively. Certain nodes in V are DCs, each of which carries the multidimensional IT resources (e.g., CPU cycles, memory, and disk storage) as

$$C_v = \langle c_{v,1}, c_{v,2}, \ldots, c_{v,n} \rangle, \quad \forall v \in V_r, \tag{1}$$

where C_v is the IT resource vector of node v, $c_{v,i}$ represents the ith IT resource that is available in v, n is for the total number of IT resource types, and V_r refers to the set of DC nodes in the EO-DCI ($V_r \subseteq V$). In the physical layer, each fiber link $e \in E$ carries F FSs as its spectrum resource.

In the EO-DCI, a connection request can be modeled as $R_j(s_j, b_j, W_j)$, where j is the unique index of the request, $s_j \in V$ is the source node, b_j is the bandwidth requirement in FSs, and W_j is the IT resource requirement of R_j, which is also a vector, as

$$W_j = \langle w_{j,1}, w_{j,2}, \ldots, w_{j,n} \rangle, \tag{2}$$

where $w_{j,i}$ denotes the requirement on the ith IT resource in the destination DC. Here, we assume that all the requests can be served with anycast, and thus the destination DC is not specified by the request. It is known that for the requests in optical DCIs, the requirements on IT resources generally scale linearly with their bandwidth demands [23]. But the actual requirements on different types of IT resources, i.e., $\langle w_{j,1}, w_{j,2}, \ldots, w_{j,n} \rangle$, can vary among the requests. For instance, the authors of [2] surveyed the IT resource requirements of applications in optical DCIs, and mentioned the existence of CPU- and storage-dominant requests. Therefore, we assume that the requirements on bandwidth and IT resources have the following relation:

$$W_j = \vec{\alpha} \cdot b_j + \vec{\zeta}, \tag{3}$$

where $\vec{\alpha}$ and $\vec{\zeta}$ are two n-dimensional vectors; $\vec{\alpha}$ is a constant one that represents the linear relation, while $\vec{\zeta}$ is a variable vector that is selected randomly within a range for each R_j to model the uncertainty in reality.

With the aforementioned network model, the request provisioning in EO-DCIs requires a procedure that can accomplish two things: 1) determining the destination DC $d_j \in V_r$ that can supply sufficient IT resources to satisfy W_j, and 2) calculating the RSA result for the lightpath from s_j to d_j to allocate enough spectrum resources. For simplicity, we assume that each R_j is served with one DC, and single-path routing is applied to set up the lightpath from s_j to d_j. We also assume that there are no spectrum converters in the EO-DCI, and all the lightpaths should be provisioned all-optically end-to-end.

B. Fragmentation of Multidimensional Resources

On the fiber links of the EO-DCI, spectrum fragmentation can occur when the lightpaths are set up and torn down frequently [12,13]. Meanwhile, as the IT resources in each DC are multidimensional, unbalanced usage can lead to the fragmentation of IT resources [17]. Moreover, the mismatch between the availability of spectrum and IT resources can also cause network performance degradation. Figure 1 shows an intuitive example of the multidimensional resource fragmentation in EO-DCI. On *nodes* 2 and 5, we have two DCs whose IT resource usage is also shown. Here, we assume $n = 3$ and consider three types of IT resources as CPU cycle, memory, and disk storage in each DC. It can be seen that the memory in *node* 2 has been used up, and thus its IT resources are fragmented. Therefore, we cannot route the request from *node* 1 to *node* 2, even though the CPU and storage resources are plentiful and the spectrum resource on *link* $1 \to 2$ is enough. On the other hand, if we select *node* 5 as the destination DC, the spectrum resources on *links* $1 \to 6$ and $6 \to 5$ are also fragmented such that there are no common available FSs on them. Hence, the request cannot be routed to *node* 5 either. Consequently, due to the multidimensional resource fragmentation, the EO-DCI blocks the request from *node* 1. Hence, the joint DF that reoptimizes the allocations of the spectrum and IT resources in EO-DCIs simultaneously is desired for better utilization of the network resources.

In order to realize the joint DF, we first need to quantify the fragmentation of multidimensional resources in an EO-DCI. Hence, two empirical metrics are defined as below, and their effectiveness will be verified with simulations.

Definition: For a link $e \in E$, we use a bit mask b_e to indicate the frequency slot (FS) usage on it. Here, if the ith FS on e is available, $b_e[i] = 0$; otherwise, $b_e[i] = 1$. Hence, $\mathrm{sum}(b_e)$ returns the total FS usage on e. We define the **spectrum fragmentation ratio (SFR)** on a link $e \in E$ as [24]

$$\phi_e = \begin{cases} 1 - \frac{\mathrm{MaxBlock}(b_e)}{F - \mathrm{sum}(b_e)}, & \mathrm{sum}(b_e) < F, \\ 0, & \mathrm{sum}(b_e) = F, \end{cases} \tag{4}$$

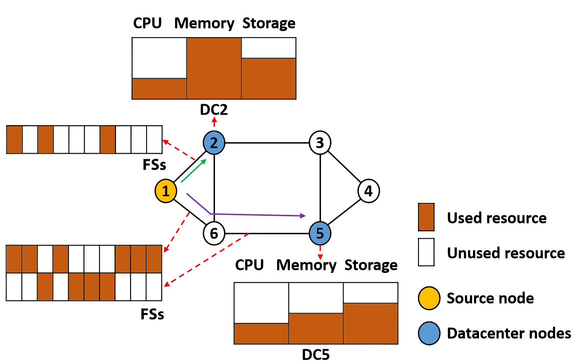

Fig. 1. Example of fragmentation of multidimensional resources in an EO-DCI.

where $\mathrm{MaxBlock}(b_e)$ returns the size of the largest available FS block (i.e., a block of spectrally contiguous FSs) on link e. The SFR can be used to measure the spectrum fragmentation on fiber links, and a larger ϕ_e means that the spectrum fragmentation on e is more severe.

Definition: We define the **IT resource fragmentation ratio (ITFR)** in a DC $v \in V_r$ as

$$p_v = \left(\prod_{i=1}^{n} \frac{c_{v,i}}{c_i^{\max}} \right)^{-\frac{1}{n}}, \qquad v \in V_r, \tag{5}$$

where $c_{v,i}$ represents the ith IT resource that is available in v, and $c_i^{\max}$ is for the maximum capacity of the ith IT resource in all the DCs in V_r. Basically, p_v leverages the geometric mean of all the normalized capacities of the IT resources in v to obtain the dimensionality reduction of its IT resource usage. Apparently, if the capacity of one type of IT resource in v approaches 0, p_v would become abnormally large. Hence, ITFR can measure the IT resource fragmentation in v, and a larger p_v means that the resources are more fragmented.

III. Joint Defragmentation

A. Overall Procedure

The joint DF considers the network reconfiguration that reallocates both the spectrum and IT resources in the EO-DCI. In order to control the operational cost and complexity, we perform the DF operation periodically, when a fixed number of requests has expired in the network.

Algorithm 1 Overall Procedure of Joint DF

1 **while** *the EO-DCI is operational* **do**
2   **if** *M requests have been expired* **then**
3   select $\lceil \rho \cdot |\mathcal{R}| \rceil$ in-service requests to reconfigure;
4   **for** *each selected request in descending order of bandwidth requirement* **do**
5   reconfigure the request;
6   **end**
7   **end**
8 **end**

Algorithm 1 shows the overall procedure of joint DF, which includes two major steps. The first one is shown in *line* 3, which selects a certain portion of the in-service requests to reconfigure. In order to avoid unnecessary operational complexity and service interruption, we need to design the request selection strategies that can find the most "critical" requests to reconfigure. Hence, the joint DF can be accomplished cost-effectively. Here, $\mathcal{R}$ represents the set of in-service requests in the EO-DCI, and $\rho \in (0, 1]$ is the selection ratio. Since each request uses both optical spectrum and IT resources, the request selection should consider both. We will discuss the details of the selection process in Subsection III.B. *Lines* 4–6 illustrate the second step, and it reconfigures the selected requests by reoptimizing their resource allocations. Note that here, we reconfigure the selected requests one by one in descending order of their bandwidth requirements (as in *line* 4). The rationale behind this is that according to Eq. (3), a request's requirement on IT resources scales approximately linearly with its bandwidth demand, and reconfiguring a request that has larger resource requirements first can usually alleviate the resource fragmentation better. We will address the methods for reconfiguring the selected requests in Section IV.

B. Request Selection Process

In order to consider the fragmentation of spectrum and IT resources jointly, we select the requests to reconfigure from two perspectives, i.e., the spectrum- and IT-oriented selections. Among the $[\rho \cdot |\mathcal{R}|]$ quota, we determine the ratios of spectrum- and IT-oriented selections based on the information of blocked requests in the network. Specifically, for the kth DF, we use two variables, B_{k-1}^{IT} and B_{k-1}^{S}, to record the numbers of requests that have been blocked due to insufficient IT and spectrum resources since the $(k-1)$th DF, respectively. Then, the ratio of spectrum-oriented selection in the kth DF can be obtained as

$$\delta_k = \frac{B_{k-1}^{S}}{B_{k-1}^{S} + B_{k-1}^{\mathrm{IT}}}, \tag{6}$$

while the ratio of IT-oriented selection is $(1 - \delta_k)$. The rationale behind this is that if more requests have been blocked due to insufficient spectrum resources, the spectrum fragmentation is more severe and we should increase the spectrum-oriented selection ratio to relieve it, and *vice versa*.

With the selection ratios determined, we find the in-service requests to reconfigure by conducting spectrum- and IT-oriented selections. For the spectrum-oriented selection, we sort the in-service requests according to their highest used FS indices (HU-FSIs), and then select $[\rho \cdot \delta_k \cdot |\mathcal{R}|]$ requests whose HU-FSIs are the highest. This is because we use the "push to the wall" scheme for spectrum DF, i.e., trying to consolidate the spectrum usage to the lower spectral end [16]. The IT-oriented selection finds the requests such that reconfiguring them can reduce the ITFRs of their DCs down to the average level. Specifically, we calculate the ITFR of each DC $v \in V_r$ with Eq. (5), and obtain the average ITFR of all the DCs as

$$p_{\mathrm{avg}} = \frac{1}{|V_r|} \sum_{v \in V_r} p_v. \tag{7}$$

Then, for each DC $v \in V_r$ in descending order of p_v, we select the requests that are causing IT resource fragmentation in it and reconfigure them to some other DCs until its new ITFR satisfies $p_v \le p_{\mathrm{avg}}$. If the number of the selected requests is less than $[(1 - \delta_k) \cdot \rho \cdot |\mathcal{R}|]$, we repeat these operations until enough requests are selected. *Algorithm 2* illustrates the detailed procedure of the request selection process.

Algorithm 2 Request Selection Process

$N = 0$
for *each in-service request in descending order of HU-FSI* **do**
  mark the request as selected;
  $N = N + 1$;
  if $N = [\delta_k \cdot \rho \cdot |\mathcal{R}|]$ **then**
    break;
  end
end
for *each* $v \in V_r$ **do**
  calculate p_v with Eq. (5);
end
while $N < [\rho \cdot |\mathcal{R}|]$ **do**
  calculate p_{avg} with Eq. (7);
  for *each DC node* $v \in V_r$ *that has* $p_v \ge p_{avg}$ *in descending order of* p_v **do**
    find the ith IT resource for which $\frac{c_{v,i}}{c_i^{max}}$ is the least;
    select the request that uses the most ith IT resource in v;
    mark the request as selected;
    $N = N + 1$;
    calculate p_v for v without the request;
    if $p_v < p_{avg}$ **or** $N = [\rho \cdot |\mathcal{R}|]$ **then**
      break;
    end
  end
end

IV. Network Reconfiguration

After selecting the in-service requests, the joint DF performs the following two things to accomplish the network reconfiguration: 1) selecting a new destination DC for each selected request to migrate its VM service, and 2) calculating a new RSA scheme to establish the network connection. The objective of the network reconfiguration is to reduce the multidimensional resource fragmentation in the EO-DCI. Hence, the problem of network reconfiguration essentially becomes how to reprovision the selected requests with multidimensional resources in a nonempty EO-DCI.

A. MILP Formulation

We first formulate an MILP model to solve the problem of network reconfiguration.

Notations:

- $G(V, E)$: Physical topology of the EO-DCI.
- V_r: Set of DC nodes in the network.
- $\mathcal{R}_s$: Set of selected requests for reconfiguration.
- $R_j(s_j, b_j, W_j)$: A selected request, $R_j \in \mathcal{R}_s$.
- $V_{r,j}$: Set of feasible destination DCs for the selected request $R_j \in \mathcal{R}_s$.
- $c_{v,i}$: Available ith IT resource in $v \in V_r$.
- $c_i^{\max}$: Maximum capacity of the ith IT resource in all the DCs in V_r.

- n: Number of IT resource types.
- F: Number of FSs on each link $e \in E$.
- $P_{u,v}$: Set of K shortest routing paths from u to v, where $u, v \in V$ and $|P_{u,v}| = K$.
- $G_{p,j}$: Set of available FS blocks for R_j on a path p, where $p \in P_{s_j,v},\ v \in V_r$. Here, each FS block contains b_j FSs.
- $L_{v,j}$: Set of feasible RSA solutions for R_j when using destination DC v. Each element $l \in L_{v,j}$ is a tuple (p, g) for a path $p \in P_{s_j,v}$ and an available FS block $g \in G_{p,j}$.
- L_j: Set of feasible RSA solutions for R_j, $L_j = \bigcup_{v \in V_r} L_{v,j}$.
- $\tilde{z}_{e,f}$: Boolean that equals 1 if the fth FS on link $e \in E$ is occupied in the network, and 0 otherwise.

Variables:

- $f^{\max}$: Integer variable that indicates the HU-FSI in the network.
- $c^a_{v,i}$: Nonnegative variable that indicates the available ith IT resource in $v \in V_r$ after reconfiguration.
- $\mu_v^{\max}$: Nonnegative variable that indicates the maximum available ratio of one type of IT resource in $v \in V_r$.
- $\mu_v^{\min}$: Nonnegative variable that indicates the minimum available ratio of one type of IT resource in $v \in V_r$.
- $\mu_i^{\max}$: Nonnegative variable that indicates the maximum available ratio of the ith IT resource among all DCs.
- $\mu_i^{\min}$: Nonnegative variable that indicates the minimum available ratio of the ith IT resource among all DCs.
- $x_{v,j}$: Boolean variable that equals 1 if request R_j chooses v as its destination DC, and 0 otherwise.
- $y_{l,j}$: Boolean variable that equals 1 if request R_j uses RSA solution l, and 0 otherwise.
- $z_{e,f}$: Boolean variable that equals 1 if the fth FS on link e is used, and 0 otherwise.
- z_f: Boolean variable that equals 1 if the fth FS is used on any link in the network, and 0 otherwise.

Objective:

The objective is to minimize HU-FSI and balance the usage of IT resources in the EO-DCI. We define two metrics to describe the IT resource availability in the network as follows:

$$\eta_1 = \sum_{v \in V_r} (\mu_v^{\max} - \mu_v^{\min}), \tag{8}$$

$$\eta_2 = \sum_{i=1}^{n} (\mu_i^{\max} - \mu_i^{\min}). \tag{9}$$

Then, the optimization objective can be formulated as

$$\text{Minimize}\left(\frac{f^{\max}}{F} + \beta \cdot \eta_1 + \gamma \cdot \eta_2\right), \tag{10}$$

where β and γ are the constants to normalize the terms according to their importance. The first item is about the HU-FSI in the network, which reflects the spectrum fragmentation. Basically, for the same amount of bandwidth demands, a smaller $f^{\max}$ means that the spectrum allocations are organized in a more compact manner. The second term quantifies the balancing of the IT resource usage in each DC, while the last one is about the balancing of the IT resource usage among all DCs. As unbalanced IT resource usage leads to fragmentation, smaller values from the last two terms suggest that the IT resources are less fragmented.

Constraints:

1) Destination selection constraints:

$$\sum_{v \in V_{r,j}} x_{v,j} = 1, \quad \forall R_j \in \mathcal{R}_s. \tag{11}$$

Equation (11) ensures that each request R_j has to be served to avoid service disruption after the reconfiguration.

2) Spectrum assignment constraints:

$$\sum_{l \in L_{v,j}} y_{l,j} = x_{v,j}, \quad \forall\ R_j \in \mathcal{R}_s, \quad \forall\ v \in V_{r,j}. \tag{12}$$

Equation (12) ensures that each request uses one and only one RSA:

$$\sum_{R_j} \sum_{l \in L_j} y_{l,j} \le (z_{e,f} + \tilde{z}_{e,f}),\ l = (p, g), \quad \forall e \in p, \quad \forall f \in g, \tag{13}$$

$$\sum_{R_j} \sum_{l \in L_j} y_{l,j} \ge z_{e,f},\ l = (p, g), \quad \forall e \in p, \quad \forall f \in g, \tag{14}$$

$$z_{e,f} + \tilde{z}_{e,f} \le 1, \quad \forall e \in E, \quad \forall f \in F. \tag{15}$$

Equations (13)–(15) ensure that the new RSA selections for all the requests satisfy the spectrum nonoverlapping constraint.

3) IT resource assignment constraints:

$$\sum_{R_j} w_{j,i} \cdot x_{v,j} \le c_{v,i}, \quad \forall v \in V_{r,j}, \quad \forall i \in [1, n]. \tag{16}$$

Equation (16) ensures that the assigned IT resource will not exceed the available capacity in one DC:

$$c^a_{v,i} = c_{v,i} - \sum_{R_j} w_{j,i} \cdot x_{v,j}, \quad \forall\ v \in V_{r,j}, \quad \forall\ i \in [1, n]. \tag{17}$$

Equation (17) calculates the available IT resource in a DC after the reconfiguration.

4) Other constraints:

$$z_f \ge (z_{e,f} + \tilde{z}_{e,f}), \quad \forall\ e \in E, \quad \forall\ f \in F. \tag{18}$$

Equation (18) ensures that the FS usage on a link is correctly recorded:

$$f^{\max} \ge f \cdot z_f, \quad \forall\ f \in F. \tag{19}$$

$$\mu_v^{\max} \geq \frac{c_{v,i}^a}{c_i^{\max}}, \quad \forall\, v \in V_r, \quad \forall\, i \in [1,n], \tag{20}$$

$$\mu_v^{\min} \leq \frac{c_{v,i}^a}{c_i^{\max}}, \quad \forall\, v \in V_r, \quad \forall\, i \in [1,n], \tag{21}$$

$$\mu_i^{\max} \geq \frac{c_{v,i}^a}{c_i^{\max}}, \quad \forall\, i \in [1,n], \quad \forall\, v \in V_r, \tag{22}$$

$$\mu_i^{\min} \leq \frac{c_{v,i}^a}{c_i^{\max}}, \quad \forall\, i \in [1,n], \quad \forall\, v \in V_r. \tag{23}$$

Equations (19)–(23) ensure that the corresponding variables are obtained correctly.

B. Heuristics for Network Reconfiguration

The MILP model can obtain the optimal reconfiguration scheme based on the network status, but due to its high computational complexity, it can only be applied to small-scale problems. Hence, in this subsection, we propose several time-efficient heuristics for network reconfiguration.

Definition: For a selected request $R_j(s_j, b_j, W_j)$, we define the **joint reconfiguration metric (JRM)** to measure the cost of selecting $v \in V_{r,j}$ as the new destination DC and using the kth path candidate from s_j to v as the new routing path:

$$h_{s_j,v,k} = (p_v \cdot q_{s_j,v,k})^{\frac{1}{2}}, \tag{24}$$

where p_v is the ITFR of the DC and can be calculated with Eq. (5), and $q_{s_j,v,k}$ is used to measure the cost of using the kth path candidate. $h_{s_j,v,k}$ is the geometric mean of p_v and $q_{s_j,v,k}$. The methods for calculating $q_{s_j,v,k}$ are discussed below.

Algorithm 3 shows the proposed overall procedure for reconfiguring a selected request $R_j(s_j, b_j, W_j)$ with the help of the JRM. Note that for *Line* 4, we consider several methods for calculating $q_{s_j,v,k}$, each of which corresponds to a heuristic.

Algorithm 3 Request Reconfiguration Based on JRM

1 **for** *each* $v \in V_{r,j}$ **do**
2   calculate ITFR p_v with Eq. (5);
3   **for** *each* $k \in [1, K]$ **do**
4   calculate $q_{s_j,v,k}$ for the kth path candidate from s_j to v;
5   calculate JRM $h_{s_j,v,k}$ with Eq. (24);
6   **end**
7 **end**
8 find the DC-path pair that has the minimum JRM;
9 select the DC-path pair;
10 reconfigure R_j to the DC-path pair;

1) Shortest-Path and ITFR-Aware Algorithm: We first consider a shortest-path and ITFR-aware algorithm (SP-ITFRA). It only considers the hop count of the kth path candidate from s_j to v when calculating $q_{s_j,v,k}$, since the path that has the smallest hop count consumes the fewest FSs in total:

$$q_{s_j,v,k} = \text{hops}(p_{s_j,v}^k), \tag{25}$$

where hops(·) returns the hop count of a path. Then, with Eqs. (24) and (25), SP-ITFRA reconfigures the request to use the DC that has low ITFR and the path that is short.

2) Fragmentation-, Misalignment-, and ITFR-Aware Algorithm: Previously in [16,25], we have demonstrated that by using the fragmentation- and misalignment-aware RSA, the blocking probability in an EON can be effectively reduced. Hence, we leverage the work in [25] to calculate $q_{s_j,v,k}$,

$$q_{s_j,v,k} = \text{cost}(p_{s_j,v}^k), \tag{26}$$

where cost(·) returns the RSA cost of a path as defined in [25]. Then, we have a fragmentation-, misalignment-, and ITFR-aware algorithm (FMA-ITFRA) that tries to minimize the fragmentation of spectrum and IT resources simultaneously.

3) Spectrum-Usage- and ITFR-Aware Algorithm: For the spectrum-usage- and ITFR-aware algorithm (SUA-ITFRA) algorithm, we calculate $q_{s_j,v,k}$ as

$$q_{s_j,v,k} = \frac{\text{FSI}_k}{F - \text{sum}(b_{p^k})} \cdot \text{hops}(p_{s_j,v}^k), \tag{27}$$

where b_{p^k} is the bit mask to indicate the FS usage on the kth path candidate $p_{s_j,v}^k$, and FSI_k is the starting index of the assigned FS block if the request R_j uses path $p_{s_j,v}^k$. Here, if the ith FS on $p_{s_j,v}^k$ is available, $b_{p^k}[i] = 0$; otherwise, $b_{p^k}[i] = 1$. Hence, $\text{sum}(b_{p^k})$ returns the total FS usage on $p_{s_j,v}^k$ before serving R_j. The rationale behind Eq. (27) is that we try to select the shortest path that is the least occupied. Basically, if path $p_{s_j,v}^k$ provides a relatively large FSI_k and its FS usage is high, we think that it is crowded and not suitable for defragmentation. Figure 2 shows several examples for calculating $q_{s_j,v,k}$ in SUA-ITFRA. We assume that R_j needs two FSs and there are three path candidates for it.

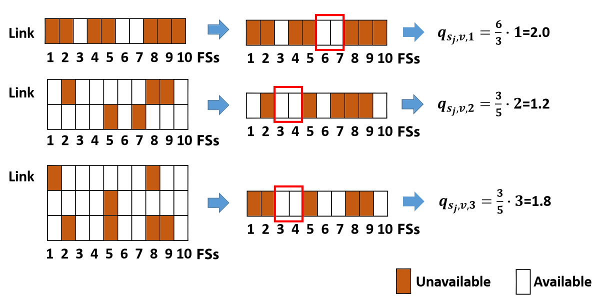

Fig. 2. Examples for calculating $q_{s_j,v,k}$ in SUA-ITFRA.

V. Performance Evaluation

In this section, we use numerical simulations to evaluate the performance of the proposed joint DF algorithms for EO-DCIs. For a request $R_j(s_j, b_j, W_j)$, the bandwidth requirement b_j is uniformly distributed within [1, 8] FSs, while the IT resource requirement W_j is determined with Eq. (3). Here, we consider three types of IT resources in each DC $v \in V_r$, i.e., CPU cycles, memory, and disk storage. When obtaining the actual requirements regarding CPU, memory, and storage, we change $\vec{\alpha}$ and $\vec{\zeta}$ in Eq. (3) to randomly generate CPU-dominant, memory-dominant, and storage-dominant requests. The details of simulation parameters are listed in Table I. Note that the initial capacities of each DC on the IT resources are randomly chosen, but we make the average values proportional to the spectrum capacity on each fiber link based on Eq. (3). This is because if the available spectrum and IT resources are not proportional, we may not need to perform the joint DF. For instance, if the IT resources in DCs are plentiful and will not be used up even when the spectrum resources are all occupied, we do not need to worry about IT resource fragmentation in the EO-DCI. Similar to those in previous studies on optical DCIs [4,23,26,27], we generate the requests according to the Poisson traffic model and quantify the traffic load in Erlangs.

In each dynamic simulation, we process 20,000 dynamic requests, and a joint DF operation is triggered when a fixed number of requests has expired in the network. Here, we use the trigger ratio (TR) to model the frequency of the joint DF operations. For example, a TR as 1% means that we invoke a joint DF every time 200 requests have expired in the network. The DF selection ratio is normally set as $\rho = 0.3$, and we also simulate different values for ρ. For the EO-DCI, we assume that all the nodes are DC nodes, i.e., $V_r = V$.

A. Performance Evaluation in a Small-Scale Network

We first run simulations in a small-scale network that has a random topology with eight nodes and 14 links [as shown in Fig. 3(a)], which is generated by the GT-ITM tool [28]. We assume that there are 100 FSs on each fiber link and the initial capacity of each DC on one type of IT resource is uniformly distributed within [80, 480] units. Other simulation parameters are explained in Table I. We simulate the scenarios with and without DF. For the scenario with DF, we compare the performance of MILP, SP-ITFRA, FMA-ITFRA, and SUA-ITFRA. We also design several benchmark algorithms to investigate the effectiveness of joint DF. For instance, if we only perform DF on the IT resources, the spectrum-oriented selection ratio will be set as $\delta_k = 0$ and the JRM in Eq. (24) is modified to $h_{s_j,v,k} = p_v$. After these modifications, we can still use the procedure of joint DF discussed in Subsection IV.B, and the corresponding benchmark algorithm is named as IT-DF. Similarly, if we only perform DF on the spectrum resources, the spectrum-oriented selection ratio will be set as $\delta_k = 1$, and the JRM in Eq. (24) is modified to $h_{s_j,v,k} = q_{s_j,v,k}$. Then, the corresponding benchmark algorithms are named SP-S-DF, FMA-S-DF, and SUA-S-DF, respectively.

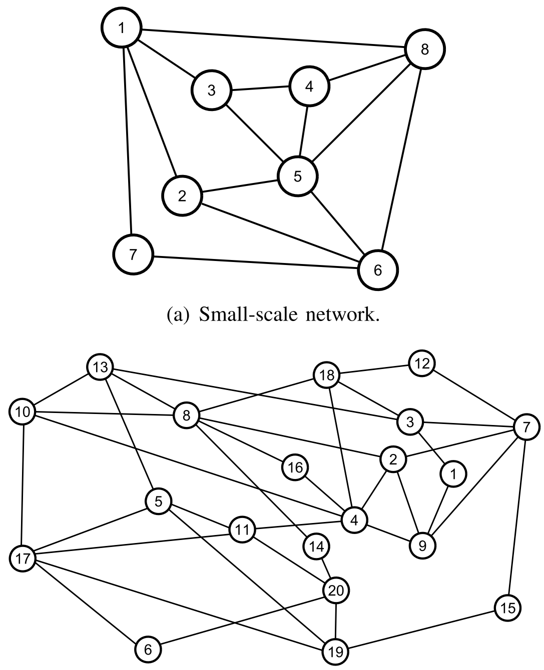

(a) Small-scale network.

(b) Large-scale network.

Fig. 3. Network topologies used in simulations.

In the simulations with the small-scale network, we generate requests with the traffic load at 40 Erlangs and invoke the DF operations with a TR of 1% and $\rho = 0.3$. Due to the complexity of the MILP, we take the results from eight DF operations and average them to get those shown in Table II. Here, we use three metrics to evaluate the performance of the algorithms, i.e., the maximum used FS index in the network (MSI), the SFR defined in Eq. (4), and the ITFR defined in Eq. (5). For each metric, we show both the maximum and average values. First of all, we can see that compared with the one without DF, all the DF algorithms can reduce some or all of the three metrics, which verifies the effectiveness of DF. IT-DF achieves the largest reduction on ITFR, but shows almost no improvement on MSI and SFR. This is because IT-DF only focuses on reducing the IT resource fragmentation. On the other hand, the DF algorithms that only perform spectrum DF, i.e., SP-S-DF, FMA-S-DF, and SUA-S-DF, can reduce MSI and SFR significantly but cannot reduce ITFR effectively.

The joint DF algorithms can reduce all three metrics simultaneously. Clearly, there is a tradeoff among the three metrics, and this is the reason SP-ITFRA, FMA-ITFRA, SUA-ITFRA, and MILP have different improvements on them. Among the four joint DF algorithms, the MILP does not provide the best results on any metrics, but it achieves the best tradeoff among the maximum MSI, maximum SFR, maximum ITFR, and average ITFR. However, it is interesting to notice that the MILP cannot reduce the average MSI and SFR effectively. This is because the objective of MILP cannot guarantee so. For instance, a request may

TABLE I
SIMULATION PARAMETERS

	Small-Scale Network	Large-Scale Network
Topology	8 nodes, 14 links	20 nodes, 37 links
F, FSs on each link	100	200
$c_{v,i}$, IT resource in a DC	[80, 480] units	[160, 960] units
b_j, requested bandwidth	[1, 8] FSs	
W_j, requested IT	$\vec{\zeta} = \langle \zeta_1, \zeta_2, \zeta_3 \rangle, \quad \zeta_i \in [1, 10]$ units CPU-dominant: $\vec{\alpha} = \langle 4, 0.5, 0.5 \rangle$ Memory-dominant: $\vec{\alpha} = \langle 0.5, 4, 0.5 \rangle$ Storage-dominant: $\vec{\alpha} = \langle 0.5, 0.5, 4 \rangle$	

choose the path that has more hop counts when two feasible ones result in the same maximum MSI in the network, and this can potentially increase the values of average MSI and SFR.

B. Performance Evaluation in a Large-Scale Network

We now evaluate the joint DF algorithms with dynamic network operations that use a large-scale topology. Figure 3(b) shows the topology, which has 20 nodes and 37 links and is still randomly generated by the GT-ITM tool. This time, we have 200 FSs on each fiber link, and the initial capacity of each DC on one type of IT resource is uniformly distributed within [160, 960] units.

1) Spectrum and IT Resource Fragmentation: First, we observe the changes of certain metrics that are related to spectrum and IT resource fragmentation (i.e., average MSI, SFR, and ITFR in the EO-DCI) in one simulation. Specifically, we fix the traffic load at 300 Erlangs, run the simulation with dynamic requests, and plot the changes of these metrics over the simulation time. In Figs. 4(a) and 4(b), we observe that SUA-S-DF and SUA-ITFRA provide smaller results on average MSI and SFR than IT-DF. This is because SUA-S-DF and SUA-ITFRA consider spectrum DF and can reduce spectrum fragmentation in the EO-DCI. Meanwhile, in Fig. 4(c), the results on average ITFR from IT-DF are the smallest, which verifies the effectiveness of IT-DF in relieving IT fragmentation. Moreover, Fig. 4(c) also indicates that the average ITFR from SUA-ITFRA is generally smaller than that from SUA-S-DF, and this confirms that SUA-ITFRA achieves joint DF of spectrum and IT resources.

2) Blocking Probability: Figure 5 shows the simulation results on blocking probability. Figures 5(a)–5(c) compare the results from without DF, with IT DF only, with spectrum DF only, and with joint DF. In each figure, we consider one routing scheme for the scenarios with spectrum DF only and joint DF. With these three figures, we can see that compared with the scenario without DF, those with DF reduce the blocking probability.

When there is IT DF only (i.e., IT-DF), the improvement in blocking performance is the smallest, which suggests that we cannot only address IT resource fragmentation in the EO-DCI. Basically, Since IT-DF only addresses IT resource fragmentation, it cannot make better use of the spectrum resources. The small improvement in blocking performance can also be expected from the fragmentation results in Table II and Fig. 4. On the other hand, if we only apply the spectrum DF (i.e., SP-S-DF, FMA-S-DF, and SUA-S-DF), the curves in Figs. 5(a)–5(c) show that the improvement in blocking performance is larger, which suggests that spectrum fragmentation is the major factor in limiting the EO-DCI's blocking performance. As expected, the proposed joint DF algorithms (i.e., SP-ITFRA, FMA-ITFRA, and SUA-ITFRA) provide the best blocking performance in each figure since they alleviate the fragmentation on multidimensional resources simultaneously. Basically, the joint DF considers both spectrum and IT resource fragmentation and tries to reduce them in an adaptive manner, and thus it can use the multidimensional resources in the EO-DCI to accommodate the most requests.

To compare the performance of the joint DF algorithms, Fig. 5(d) plots their results on blocking probability together. We observe that their performance is similar, but FMA-ITFRA performs slightly better than SP-ITFRA and SUA-ITFRA. Basically, since FMA-ITFRA addresses spectrum fragmentation the best in routing path selection, it can

TABLE II
RESULTS FROM SIMULATIONS WITH THE SMALL-SCALE NETWORK (40 ERLANGS)

	Without DF	IT-DF	SP-S-DF	FMA-S-DF	SUA-S-DF	SP-ITFRA	FMA-ITFRA	SUA-ITFRA	MILP
Maximum MSI	42.13	42.13	28.88	20.75	20.50	28.63	24.63	23.63	23.88
Average MSI	17.07	16.33	8.81	8.73	9.09	10.28	10.18	10.22	15.98
Maximum SFR	0.59	0.55	0.26	0.24	0.23	0.35	0.32	0.31	0.40
Average SFR	0.18	0.16	0.05	0.05	0.04	0.07	0.07	0.05	0.17
Maximum ITFR	7.67	3.74	10.40	6.75	6.98	4.78	4.89	5.68	4.86
Average ITFR	3.20	2.40	3.64	3.10	3.11	2.63	2.67	2.88	2.67

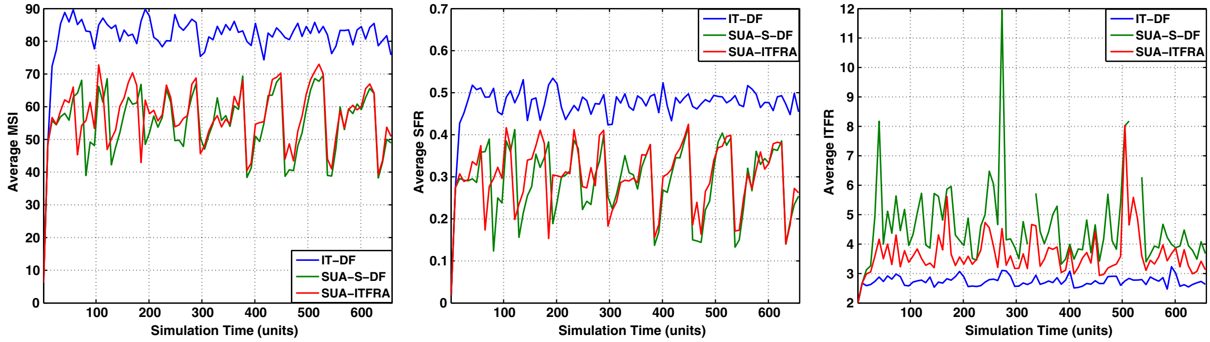

(a) Results on average MSI. (b) Results on average SFR. (c) Results on average ITFR.

Fig. 4. Results on spectrum and IT resource fragmentation over simulation time (300 Erlangs).

handle spectrum DF most effectively and hence achieves the best blocking performance. SUA-ITFRA also considers spectrum fragmentation in routing path selection, and thus its blocking performance is better than that of SP-ITFRA, except for the low traffic load cases (≤250 Erlangs). This is because for low traffic load cases, the SUA-based routing scheme cannot address spectrum fragmentation as precisely as the FMA-based one. Finally, we can conclude that even though its impact is small, the routing scheme does affect the performance of joint DF.

3) Impact of DF Selection Ratio and Trigger Ratio: In order to investigate the impact of the DF selection ratio ρ, we simulate SUA-ITFRA with ρ changing from 0.1 to 0.9. Figures 6(a) and 6(b) show the simulation results when TR is 1% and 2%, respectively. Basically, a larger ρ means

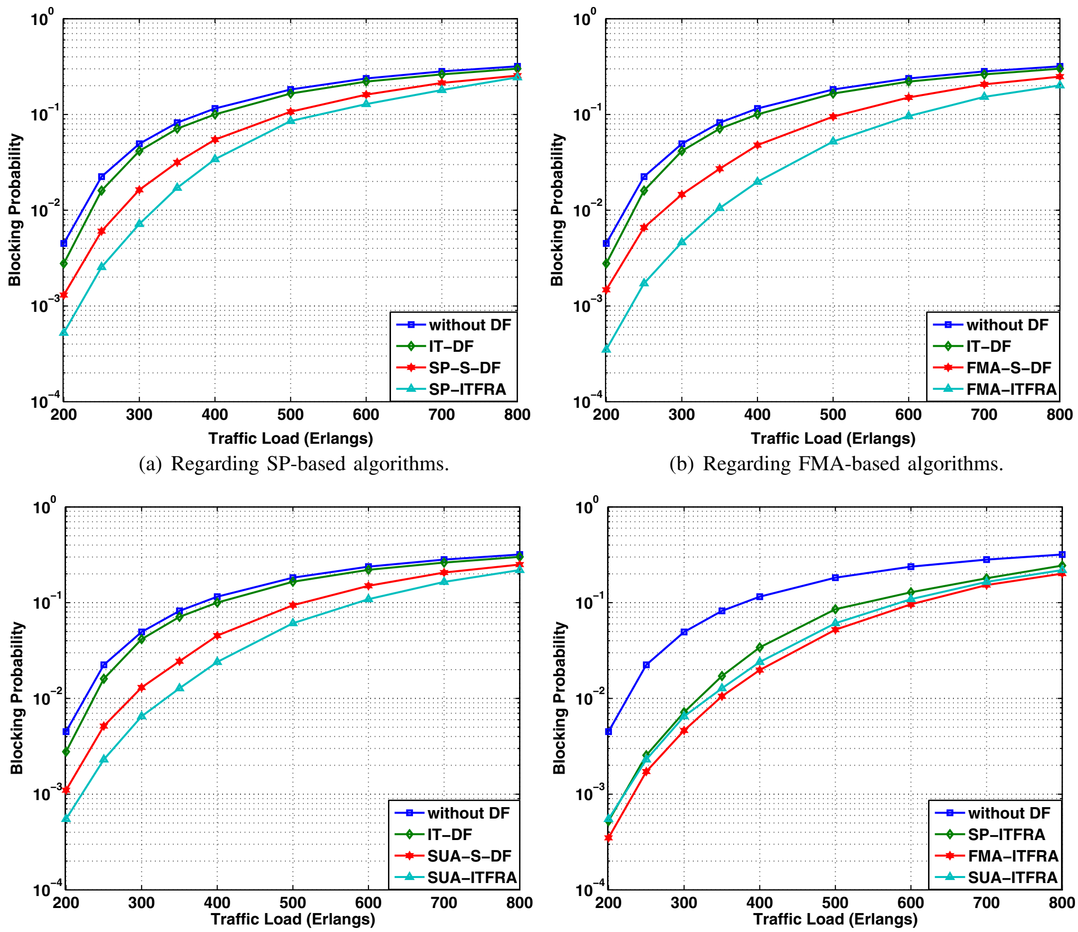

(a) Regarding SP-based algorithms. (b) Regarding FMA-based algorithms.

(c) Regarding SUA-based algorithms. (d) Overall comparison.

Fig. 5. Results on blocking probability.

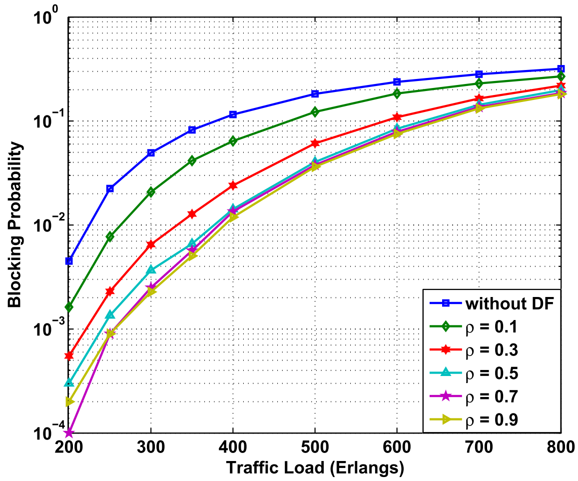

(a) With trigger ratio TR = 1%.

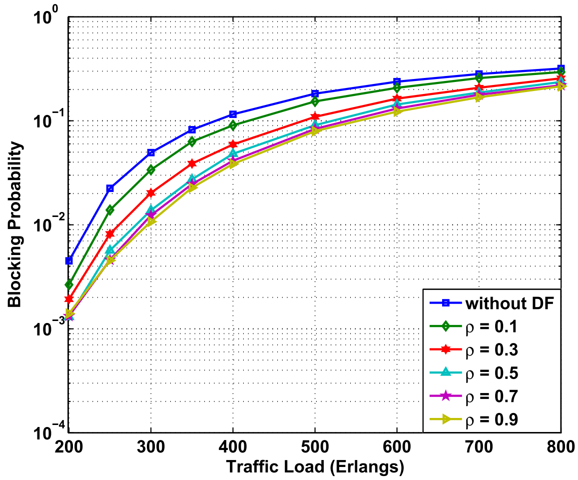

(b) With trigger ratio TR = 2%.

Fig. 6. Results on blocking probability from SUA-ITFRA.

that we can reconfigure more in-service requests in each DF operation and hence leads to better blocking performance. The results in Fig. 6 verify this. It is also interesting to notice that the reduction in blocking probability becomes smaller when ρ increases. For instance, when TR is 1%, the blocking probabilities for $\rho = 0.7$ are similar to those for $\rho = 0.9$, while for TR $= 2\%$, the curves for $\rho = 0.5$, 0.7, and 0.9 are very close. This is because we design the request selection strategy to find the most "critical" requests to reconfigure, and hence when ρ is reasonably large, the margin on blocking probability left for the joint DF to improve further is very limited.

Note that TR determines the timing of each DF operation, and a smaller TR means that the DF operations are triggered more frequently. By comparing the results in Figs. 6(a) and 6(b), we observe that ρ has a smaller impact on the blocking performance when TR is larger. This can be explained as follows. When we have TR $= 2\%$, the DF operations are not triggered as timely as with TR $= 1\%$. Therefore, even though each DF still reduces resource fragmentation, new fragmentation will be generated in the longer DF interval and limit the network performance. Or in other words, when we have TR $= 2\%$, each DF operation is invoked too late when the damage from resource fragmentation (i.e., request blocking) has already been there and can be reduced less.

Meanwhile, we should notice that when we select more in-service requests to reconfigure with a larger ρ and/or trigger the DF operations more frequently with a smaller TR, the operational complexity also increases. Therefore, in practical network operations, we should carefully consider the tradeoff between the performance improvement and operational complexity when determining the joint DF's parameters.

VI. Conclusion

In this paper, we studied the problem of joint DF for the spectrum and IT resources in EO-DCIs. Specifically, in order to reduce the blocking probability in an EO-DCI, we reoptimized the allocations of the multidimensional resources jointly with complexity-controlled network reconfigurations. For each DF operation, we first investigated the request selection process and proposed a joint selection strategy that can perform the spectrum- and IT-oriented selections adaptively according to the actual network status. Then, we formulated an MILP model and designed several heuristics to tackle the problem of network reconfiguration in the joint DF. Simulation results showed that the proposed joint DF algorithms can significantly reduce the blocking probability in EO-DCIs by consolidating the spectrum and IT resource usage effectively.

Acknowledgments

This work was supported in part by the NCET program under Project NCET-11-0884, NSFC Project 61371117, the Fundamental Research Funds for the Central Universities (WK2100060010), the Natural Science Research Project for Universities in Anhui (KJ2014ZD38), the Strategic Priority Research Program of the CAS (XDA06010302), and the State Key Laboratory of Advanced Optical Communication Systems Networks, China.

References

[1] C. Liu, A. Kind, and A. Vasilakos, "Sketching the data center network traffic," *IEEE Netw.*, vol. 27, pp. 33–39, July 2013.

[2] C. Develder, M. De Leenheer, B. Dhoedt, M. Pickavet, D. Colle, F. De Turck, and P. Demeester, "Optical networks for grid and cloud computing applications," *Proc. IEEE*, vol. 100, pp. 1149–1167, May 2012.

[3] M. Gharbaoui, B. Martini, and P. Castoldi, "Dynamic network resource allocation for inter-data centers communications," in *Proc. OFC*, Mar. 2012, pp. 1–3.

[4] M. Gharbaoui, B. Martini, and P. Castoldi, "Anycast-based optimizations for inter-data-center interconnections," *J. Opt. Commun. Netw.*, vol. 4, pp. B168–B178, Nov. 2012.

[5] W. Cerroni, F. Callegati, B. Martini, and P. Castoldi, "Analytical model for anycast service provisioning in data center interconnections," in *Proc. ONDM*, Apr. 2012, pp. 1–6.

[6] M. Jinno, H. Takara, B. Kozicki, Y. Tsukishima, Y. Sone, and S. Matsuoka, "Spectrum-efficient and scalable elastic optical path network: Architecture, benefits, and enabling technologies," *IEEE Commun. Mag.*, vol. 47, no. 11, pp. 66–73, Nov. 2009.

[7] O. Gerstel, M. Jinno, A. Lord, and S. Yoo, "Elastic optical networking: A new dawn for the optical layer?" *IEEE Commun. Mag.*, vol. 50, no. 2, pp. s12–s20, Feb. 2012.

[8] L. Contreras, V. Lopez, O. De Dios, A. Tovar, F. Munoz, A. Azanon, J. Fernandez-Palacios, and J. Folgueira, "Toward cloud-ready transport networks," *IEEE Commun. Mag.*, vol. 50, no. 9, pp. 48–55, Sept. 2012.

[9] S. Yoo, Y. Yin, and K. Wen, "Intra and inter datacenter networking: The role of optical packet switching and flexible bandwidth optical networking," in *Proc. ONDM*, Apr. 2012, pp. 1–6.

[10] S. Peng, R. Nejabati, M. Channegowda, and D. Simeonidou, "Application-aware and adaptive virtual data centre infrastructure provisioning over elastic optical OFDM networks," in *Proc. ECOC*, Sept. 2013, pp. 1–3.

[11] M. Klinkowski and K. Walkowiak, "On the advantages of elastic optical networks for provisioning of cloud computing traffic," *IEEE Netw.*, vol. 27, pp. 44–51, Nov. 2013.

[12] T. Takagi, H. Hasegawa, K. Sato, Y. Sone, A. Hirano, and M. Jinno, "Disruption minimized spectrum defragmentation in elastic optical path networks that adopt distance adaptive modulation," in *Proc. ECOC*, Sept. 2011, pp. 1–3.

[13] M. Zhang, W. Shi, L. Gong, W. Lu, and Z. Zhu, "Bandwidth defragmentation in dynamic elastic optical networks with minimum traffic disruptions," in *Proc. ICC*, June 2013, pp. 3894–3898.

[14] A. Patel, P. Ji, J. Jue, and T. Wang, "Defragmentation of transparent flexible optical WDM (FWDM) networks," in *Proc. OFC*, Mar. 2011, pp. 1–3.

[15] R. Wang and B. Mukherjee, "Spectrum management in heterogeneous bandwidth networks," in *Proc. GLOBECOM*, Dec. 2012, pp. 2907–2911.

[16] M. Zhang, C. You, H. Jiang, and Z. Zhu, "Dynamic and adaptive bandwidth defragmentation in spectrum-sliced elastic optical networks with time-varying traffic," *J. Lightwave Technol.*, vol. 32, pp. 450–460, Feb. 2014.

[17] M. Sridharan, P. Calyam, A. Venkataraman, and A. Berryman, "Defragmentation of resources in virtual desktop clouds for cost-aware utility-optimal allocation," in *Proc. UCC*, Dec. 2011, pp. 253–260.

[18] I. Widjaja, S. Borst, and I. Saniee, "Building an elastic cloud out of small datacenters," in *Proc. CCGrid*, May 2013, pp. 10–17.

[19] W. Jia, D. Xuan, and W. Zhao, "Integrated routing algorithms for anycast messages," *IEEE Commun. Mag.*, vol. 38, no. 1, pp. 48–53, Jan. 2000.

[20] L. Gong, W. Zhao, Y. Wen, and Z. Zhu, "Dynamic transparent virtual network embedding over elastic optical infrastructures," in *Proc. ICC*, June 2013, pp. 3466–3470.

[21] J. Zhao, S. Subramaniam, and M. Brandt-Pearce, "Virtual topology mapping in elastic optical networks," in *Proc. ICC*, June 2013, pp. 3904–3908.

[22] X. Liu, L. Zhang, M. Zhang, and Z. Zhu, "Joint defragmentation of spectrum and computing resources in inter-datacenter networks over elastic optical infrastructure," in *Proc. ICC*, June 2014, pp. 3295–3300.

[23] J. Buysse, K. Georgakilas, A. Tzanakaki, M. De Leenheer, B. Dhoedt, and C. Develder, "Energy-efficient resource-provisioning algorithms for optical clouds," *J. Opt. Commun. Netw.*, vol. 5, pp. 226–239, Mar. 2013.

[24] X. Zhou, W. Lu, L. Gong, and Z. Zhu, "Dynamic RMSA in elastic optical networks with an adaptive genetic algorithm," in *Proc. GLOBECOM*, Dec. 2012, pp. 2912–2917.

[25] Y. Yin, M. Zhang, Z. Zhu, and S. Yoo, "Fragmentation-aware routing, modulation and spectrum assignment algorithms in elastic optical networks," in *Proc. OFC*, Mar. 2013, pp. 1–3.

[26] A. Nikolaidis, S. Asselin, M. Auster, and N. Bragg, "Capacity planning for dynamic inter-data center networking via Erlang modeling," in *Proc. ECOC*, Sept. 2013, pp. 1–3.

[27] A. Asensio, L. Velasco, M. Ruiz, and G. Junyent, "Carrier SDN to control flexgrid-based inter-datacenter connectivity," in *Proc. ONDM*, May 2014, pp. 43–48.

[28] E. Zegura, K. Calvert, and S. Bhattacharjee, "How to model an internetwork," in *Proc. INFOCOM*, Mar. 1996, pp. 594–602.